Journal of Materials and Construction
ISSN 2734-9438
Website: www. jomc.vn

Modified space-truss model for predicting the torsional capacity of Ultra-high-performance concrete beams

Nguyen Vu Luat[1], Nguyen Vinh Sang[2*]

[1]Smart Computing in Civil Engineering Research Group, Faculty of Civil Engineering, Ton Duc Thang University

[2]Faculty of Civil Engineering, Thuyloi University

KEYWORDS

Torsion
Torsional capacity
Ultra-high-performance concrete beam
Modified space-truss model

ABSTRACT

Ultra-high-performance concrete (UHPC) beams exhibit enhanced post-cracking stress transfer due to fiber bridging, a mechanism not adequately represented in conventional torsion design provisions. This study develops a modified space-truss model (MSTM) to predict the ultimate torsional capacity of UHPC beams under pure torsion. The proposed formulation retains the three-dimensional space-truss analogy and thin-walled tube idealization, while explicitly incorporating the tensile contribution of UHPC through equivalent longitudinal and transverse tensile components. In addition, the inclination angle of the concrete strut is refined using equilibrium and strain-compatibility considerations rather than fixed code-recommended values. The reliability of the MSTM is validated using a compiled database of 40 UHPC beams from previous experimental studies and benchmarked against the truss-based provisions in ACI 318-19 and GB 50010. The results indicate that both code-based approaches tend to provide conservative predictions. In contrast, the proposed MSTM achieves improved agreement with experiments (mean value = 0.90 for Tu,cal/Tu,exp) while remaining slightly conservative for design.

1. Introduction

Prior studies have extensively examined the flexural and shear responses of UHPC members [1, 2], their torsional response remains relatively underexplored. Traditionally, torsional demand has been addressed by increasing the ratios of transverse reinforcement (stirrups) and longitudinal reinforcement. However, the rapid adoption of advanced materials and industrialized construction has promoted structural components that are lighter, stronger, and increasingly prefabricated. At the same time, modern buildings are becoming taller, more geometrically complex, and more deformable, conditions under which torsional actions may become significant [3]. Consequently, the torsion-related performance of structural members warrants explicit consideration rather than being treated as a secondary effect.

Early experimental investigations of torsion in concrete members were initiated by Hsu [4], who performed pure torsion tests on reinforced concrete (RC) beams and clarified characteristic torsional failure mechanisms. Lopes et al. [5] extended torsion testing to high-strength concrete (HSC) hollow beams and observed that meaningful torsional ductility was achieved only within a limited range of torsional reinforcement. To facilitate practical assessment, Rahal et al. [6] proposed a non-iterative method to estimate ultimate torsional strength by combining the effects of longitudinal reinforcement, transverse reinforcement, concrete compressive strength, and cross-sectional area. Despite these advances, the inherently low tensile resistance and brittle post-cracking response of conventional concrete and HSC can constrain their suitability for torsion-critical applications.

To mitigate brittleness and enhance tensile capacity, researchers have incorporated discrete fibers into cementitious matrices, forming fiber-reinforced concrete (FRC) systems with improved crack control. Rao et al. [7] reported that steel fibers can increase both torsional strength and ductility of FRC beams, while Okay et al. [8] showed that the energy absorption capacity is strongly influenced by fiber characteristics (e.g., dosage and aspect ratio) together with the longitudinal reinforcement ratio. Karimipour et al. [9] further suggested that, for high-performance concrete beams, polypropylene fibers may provide greater improvements in torsional response than steel fibers. More recently, UHPC, a dense, steel-fiber-reinforced cementitious composite designed using particle packing concepts [10], has been increasingly adopted in bridge, building, nuclear, municipal, and marine infrastructure applications [11]. Owing to its dense matrix and pronounced fiber-bridging action, UHPC exhibits a distinct torsional response, often characterized by delayed cracking, enhanced post-cracking resistance, and improved transfer of tensile stresses across cracks relative to ordinary concrete, HSC, and conventional FRC. Existing experimental evidence indicates that the torsional performance of UHPC members is affected by fiber content and reinforcement detailing [12], cover-related failure mechanisms [13], and strengthening measures such as UHPC jacketing [14]; geometric effects on cracking torque and the benefits of flange plates on strength and twist angle have also been reported for hollow sections [15]. Hybrid

*Corresponding author: sangnv@tlu.edu.vn
Received 02/02/2026, revised 11/02/2026, accepted 13/02/2026
Link DOI: https://doi.org/10.54772/jomc.v16i01.1247

fiber systems have been shown to further increase cracking and ultimate torques [16], and a minimum fiber dosage has been suggested to establish a stable post-cracking load-carrying mechanism in conjunction with longitudinal reinforcement [17]. However, a unified and mechanics-consistent interpretation that links these observations to robust torsion design predictions remains limited, motivating further research to improve modeling and codification for UHPC members under pure torsion.

Several studies and design-oriented documents have sought to formulate practical torsion provisions for UHPC beams. Existing standards, ACI 318-19 [18] and GB 50010 [19], offer simplified expressions to estimate the cracking torque and peak (ultimate) torque; however, their applicability to UHPC is often constrained because they do not adequately represent the post-cracking tensile response of the composite or the interaction with steel reinforcement [15]. In this context, the modifications proposed by Li et al. [20] and Cao et al. [3] emphasized the importance of incorporating tensile resistance within the GB 50010 [19] framework. Likewise, Khawh et al. [21] derived refined torsion equations grounded in the thin-walled tube analogy. Despite these advances, many methods still give limited attention to the role of longitudinal reinforcement, transverse reinforcement (stirrups), and the tensile contribution of UHPC, although these factors are critical for torsional load transfer and remain insufficiently addressed in several code-based and analytical approaches.

Comparisons with international developments, such as the *fib* Model Code 2010 [22] and the ongoing revisions of Eurocode 2 [23] indicate an increasing recognition of the structural contribution of fibers in shear- and torsion-critical mechanisms. Nevertheless, explicit and comprehensive torsion design guidance tailored to UHPC members is still lacking, highlighting the need for further analytical research to support robust codification.

In this study, a modified space-truss model (MSTM) is developed to predict the torsional capacity of UHPC beams. The proposed model incorporates the tensile stress contribution of UHPC and accounts for a refined evaluation of the concrete strut inclination angle. A total of forty UHPC beams reported in previous experimental studies were compiled to verify the predictive capability of the MSTM and benchmark its performance against space-truss-based models prescribed in current design standards.

2. Space-truss models in current design standards

2.1. Standard ACI-318-19 [18]

The space-truss theory has been widely adopted worldwide to evaluate the torsional capacity of reinforced concrete members. It was first developed by Rausch [24] and subsequently refined by Lampert and Thürlimann [25], along with many other researchers. Improved versions of this theory have been incorporated into major design codes, including ACI-318-19 [18], CEB-FIP-90 [26], CAN3-A23.3-04 [27], and EN-1992-1-1:2004 [23]. In the space-truss model, it is assumed that torsion is resisted primarily by a perimeter zone of the cross-section with an effective wall thickness (t_d). Accordingly, both solid and hollow sections are idealized as an equivalent thin-walled closed section with a uniform wall thickness (t_d). A constant shear flow (q) is then assumed to develop through this effective wall thickness, consistent with Bredt's torsion theory [28] (Figure 1), and is expressed by Eq. (1).

$$q = \frac{T}{2A_o} \quad (1)$$

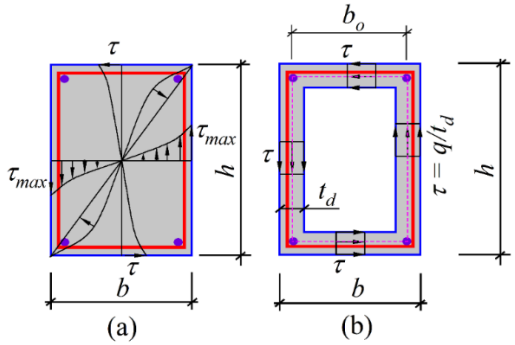

Figure 1. Shear-stress state under pure torsion: (a) elastic behavior prior to cracking, and (b) post-cracking thin-walled tube idealization.

In Eq. (1), T denotes the applied torque, and A_o is the area enclosed by the median line of the equivalent hollow section, including any internal void regions (i.e., the area associated with the shear flow). Furthermore, the walls of this equivalent hollow section are idealized using a space-truss model. The compressive concrete struts, inclined along the perimeter at an angle θ, are in equilibrium with the longitudinal and transverse tensile ties provided by the longitudinal reinforcement and transverse reinforcement (stirrups), as depicted in Figure 2. The longitudinal bars are assumed to be concentrated at the corners, whereas the transverse reinforcement is considered to be distributed along the height of the section faces. The torsional load-carrying capacity is determined from the forces in the struts, while the shear stress itself is not treated as an independent resisting component. The strut forces can be obtained from equilibrium considerations at a truss node. For simplicity, the development (unfolding) of the equivalent hollow section of a reinforced concrete beam referred to herein as the shear-wall model is adopted (Figure 2). Within this shear-wall idealization, the torsional capacity governed by the longitudinal reinforcement is expressed as follows:

$$T_{sl} = \frac{2A_o A_{sl} f_{yl}}{P_h} \tan\theta \quad (2)$$

and the torsional capacity governed by the transverse reinforcement (stirrups) is determined as follows:

$$T_{st} = \frac{2A_o A_{st} f_{yt}}{s} \cot\theta \quad (3)$$

Furthermore, ACI 318-19 [18] specifies that, under pure torsion, the torsional strength is limited by the concrete compressive capacity (T_c), which for normal-strength concrete can be expressed as follows:

$$T_c = \frac{17\sqrt{f_c'}A_{oh}^2}{12P_h} \quad (4)$$

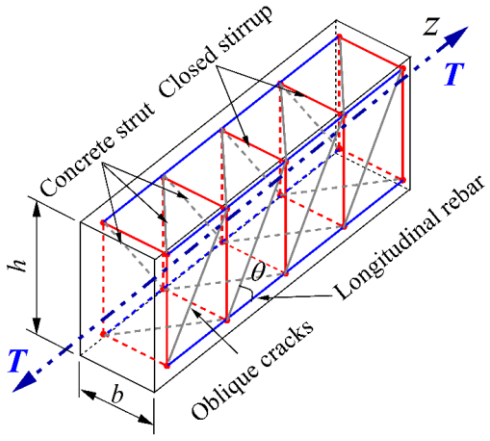

Figure 2. Post-cracking space-truss model according to ACI 318-19 [18].

where q is shear flow; f_c' is the specified cylinder compressive strength of concrete; A_{st} and A_{sl} are the area of one leg of a closed stirrup and the total area of longitudinal reinforcement, respectively; f_{yt} and f_{yl} are the yield strengths of transverse (stirrup) and longitudinal reinforcement; s is the stirrup spacing; $A_o = 0.85A_{oh}$ is the area enclosed by the shear flow; A_{oh} is the area of the core measured to the centerline of the closed stirrups; P_h is the perimeter of the core enclosed by the closed stirrups; and θ is the inclination angle of the concrete struts, varying from 30° to 60° [18]. For non-prestressed members, ACI 318-19 [18] recommends $\theta = 45°$, whereas for prestressed members $\theta = 37.5°$.

Under pure torsion, concrete is assumed not to contribute to the shear resistance ($V_c = 0$). The concrete crushing limit in the inclined struts represents an upper bound of torsional capacity, independent of the reinforcement response. The value ($T_{u,ACI}$) reflects the concrete compressive capacity under a biaxial stress state, in which concrete is compressed along the inclined struts while simultaneously subjected to tensile actions in the longitudinal and vertical directions through the longitudinal reinforcement and stirrups, respectively. Consequently, the design ultimate torsional strength is taken as the minimum of the following three values:

$$T_{u,ACI} = \min\{T_{st}, T_{sl}, T_c\} \quad (5)$$

2.2. Standard GB50010 [19]

According to GB 50010 [19], the torsional resistance of reinforced concrete members is formulated using the thin-walled tube analogy coupled with a three-dimensional space-truss model. Under pure torsion (T), the post-cracking response is idealized by an approximately uniform shear flow (q) circulating along the perimeter of a closed shear path. This shear flow is resisted by: (i) closed stirrups (transverse reinforcement) developing tensile forces in the circumferential direction, (ii) longitudinal reinforcement providing the complementary tensile tie action along the member axis, and (iii) the UHPC matrix, whose contribution is represented through an effective tensile stress that accounts for crack initiation resistance and, where applicable, residual tensile capacity associated with fiber bridging. For rectangular cross-sections, the torsion design provisions are applicable when the aspect ratio satisfies $h/b \leq 6$ [19].

For a rectangular UHPC beam subjected to pure torsion, the design torsional resistance is expressed as the sum of the UHPC contribution and the reinforcement contribution (stirrups and longitudinal bars):

$$T_{u,GB50010} = 0.7 f_{cr} w_t + 1.2\sqrt{\zeta}\frac{2A_o A_{st} f_{yt}}{s} \quad (6)$$

where f_{cr} is the cracking tensile strength of UHPC; b and h are the width and height of the rectangular cross-section, respectively. W_t is the plastic torsional section modulus of a rectangular cross-section, which is evaluated as:

$$w_t = \frac{b^2(3h-b)}{6} \quad (7)$$

Within the space-truss representation, the tensile actions carried by the closed stirrups and the longitudinal bars must satisfy equilibrium and compatibility across inclined cracking planes (Figure 5). GB 50010 [19] introduces the parameter (ζ) to quantify the relative "*strength level*" of longitudinal reinforcement versus transverse reinforcement in the torsional truss mechanism:

$$\zeta = \frac{A_{sl} f_{yl} s}{A_{st} f_{yt} u} \quad (8)$$

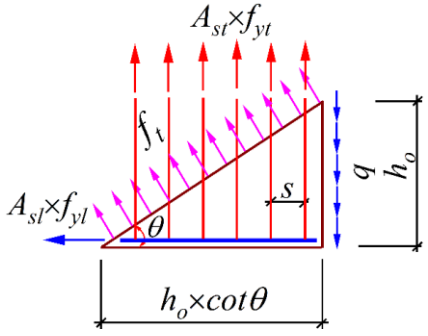

Figure 3. Stress-analysis schematic of the thin-walled tube model [19].

where u is the effective perimeter measured along the centroidal path of the shear-stress flow (τ); and ζ is equilibrium coefficient in GB 50010 torsion model.

3. Improved modified space-truss model (MSTM)

3.1. Model development

The simplified space-truss model adopted in ACI 318-19 [18] neglects the tensile resistance of UHPC; this shortcoming has been

partially improved in GB50010 [19], as presented in Section 2. Nevertheless, additional refinements are required to make the space-truss idealization more consistent with the torsion-resisting mechanism of UHPC beams. In this section, the post-cracking tensile contribution of UHPC and a revised determination of the concrete strut inclination angle θ are incorporated to modify the spacetruss models used in current design standards.

In the proposed modified space-truss model (MSTM), the ultimate torsional capacity (T_u) of UHPC beams is formulated based on the three-dimensional space-truss theory [29] together with the thin-walled tube analogy [21, 28]. The torsional resistance of UHPC beams is considered to consist of two components: the reinforcement contribution and the fiber-reinforced UHPC contribution. Within the spatial truss idealization with a strut inclination angle θ, the internal forces in the tension ties comprise the longitudinal reinforcement (chord members), the transverse reinforcement (web members, i.e., stirrups), and the inclined concrete compression struts, which are denoted by *L*, *S*, and *C*, respectively. The components of the strut force *C* in the *X* - and *Y*-directions are balanced by the transverse ties *S*, whereas the *Z*-direction component is balanced by the longitudinal ties *L*, as illustrated in Figure 4.

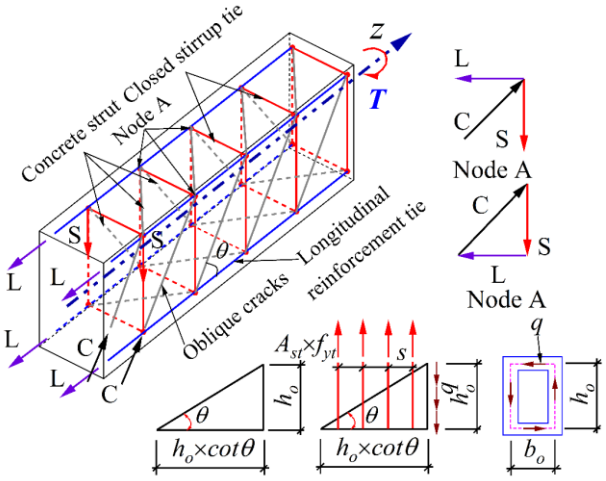

Figure 4. Analytical schematic of the proposed modified space-truss model (MSTM).

In addition, unlike conventional concrete, UHPC exhibits a superior tensile capacity; therefore, the spatial truss model should be modified to incorporate this tensile stress, which is assumed to act normal to the surface of a smooth crack (Figure 4) [21]. The UHPC tensile stress can be decomposed into two components, namely longitudinal and transverse. By interpreting their resisting effects as additional tensile ties in the longitudinal and transverse directions, the unfolded shear-wall representation of a UHPC beam shown in Figure 5 can be established [30]. Accordingly, the additional tensile tie forces provided by UHPC, denoted as F_{fl} and F_{ft}, are introduced at the truss nodes (Node A) in the nodal equilibrium of the truss system.

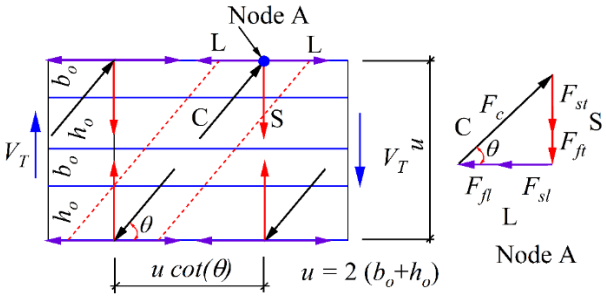

Figure 5. Nodal equilibrium including the additional tensile ties provided by UHPC.

The shear stress flow (τ) induced by pure torsion (see Eq. (1)) can be integrated over the height of the unfolded shear wall, (u), to obtain the resultant torsional shear force V_T. Here, u also represents the effective perimeter measured along the centroidal path of the shear stress flow (τ), as follows:

$$V_T = qu = \frac{Tu}{2A_o} \quad (9)$$

The applied torsional shear force is obtained from equilibrium with the contributions of the reinforcing steel (longitudinal bars and stirrups) and the tensile contribution of the UHPC component in the longitudinal and vertical directions [30]. For the additional tensile ties provided by UHPC in the longitudinal direction, the following relationship is derived from the projection of the nodal equilibrium along the longitudinal axis:

$$F_{fl} = V_T \cot\theta = \frac{Tu}{2A_o}\cot\theta \quad (10)$$

For the additional tensile ties provided by UHPC in the vertical direction:

$$F_{ft} = V_T = \frac{Tu}{2A_o} \quad (11)$$

Assuming that the resultant tensile force is uniformly distributed and acts normal to the crack surface, as illustrated in Figure 4 and Figure 5, the following expression is obtained:

$$A_{fl} = ut_d \quad (12)$$

and the effective UHPC area in tension in the vertical direction is determined as (Figure 5):

$$A_{ft} = u\cot\theta t_d \quad (13)$$

From Eqs. (10) and (12), the tensile stress acting on the inclined crack surface in the longitudinal direction can be expressed as follows:

$$\sigma_{fl} = \frac{F_{fl}}{A_{fl}} = \frac{T\cot\theta}{t_d 2A_o} \quad (14)$$

Similarly, from Eqs. (11) and (13), the tensile stress acting on the inclined crack surface in the vertical direction can be expressed as follows:

$$\sigma_{ft} = \frac{F_{ft}}{A_{ft}} = \frac{T}{t_d 2A_o\cot\theta} \quad (15)$$

When Eqs. (14) and (15) are rewritten in terms of T, the tensile stresses can be replaced by the corresponding cracking tensile strengths of steel-fiber-reinforced concrete members in torsion ($\sigma_{fl} = f_{fl,cr}$ and $\sigma_{ft} = f_{ft,cr}$), as proposed by Oettel [30]. However, for UHPC, the tensile response may reach the ultimate tensile stress at failure [3]. Therefore, in this study, the ultimate tensile strength of UHPC is adopted ($\sigma_{fl} = f_{fl,tu}$ and $\sigma_{ft} = f_{ft,tu}$), and the torsional capacity associated with the individual struts at failure can be obtained. For the torsional strength contribution of UHPC in the longitudinal direction:

$$T_{fl} = f_{fl,tu} t_d 2A_o \tan\theta \quad (16)$$

For the torsional strength contribution of the UHPC component in the vertical direction:

$$T_{ft} = f_{ft,,tu} t_d 2A_o \cot\theta \quad (17)$$

Accordingly, the torsional capacity in each direction is taken as the sum of the contributions from the reinforcing steel (Eqs. (2) and (3)) and the UHPC component (Eqs. (16) and (17)). In the longitudinal direction, the torsional capacity is obtained by superimposing the contributions of the longitudinal reinforcement and the longitudinal UHPC component, as follows:

$$T_{sfl} = T_{sl} + T_{fl} \quad (18)$$

$$T_{sfl} = \frac{A_{sl}}{u} f_{yl} 2A_o \tan\theta + f_{fl,tu} t_d 2A_o \tan\theta \quad (19)$$

and, in the vertical direction, the torsional capacity is obtained by combining the contributions of the transverse reinforcement (stirrups) and the vertical UHPC component, as follows:

$$T_{sft} = T_{st} + T_{ft} \quad (20)$$

$$T_{sft} = \frac{A_{st}}{s} f_{yt} 2A_o \cot\theta + f_{ft,tu} t_d 2A_o \cot\theta \quad (21)$$

Because the compressive strength of concrete is only marginally affected by steel fibers [22], Eq. (5) is adopted as the compressive-limit criterion for the inclined concrete struts in UHPC subjected to pure torsion. Accordingly, in the proposed MSTM, the ultimate torsional capacity of the beam is taken as the minimum of T_{sfl}, T_{sft}, and T_c, as expressed in Eq. (22) below:

$$T_{u,MSTM} = \min\left\{T_{sft}, T_{sfl}, T_c\right\} \quad (22)$$

where V_T is the resultant torsional shear force; t_d is the effective wall thickness; $f_{fl,tu}$ and $f_{ft,tu}$ are ultimate tensile strengths of UHPC corresponding to the longitudinal and transverse components, respectively (i.e., $f_{fl,tu} = f_{ft,tu} = f_{tu}$); σ_{fl} and σ_{ft} are the longitudinal and transverse tensile stress components, respectively.

In this study, the post-cracking tensile contribution of UHPC is represented in a simplified manner using the ultimate tensile strength f_{tu}, as this parameter is commonly reported in experimental studies and enables practical implementation.

3.2. Inclination angle (θ) of the compressive concrete strut

The inclined crack angle (θ) is a key parameter for reinforced concrete members subjected to shear and torsion and can significantly affect torsional capacity [31, 32]. In this context, (θ) follows code-specific guidance for RC members under pure torsion [18, 23, 33] and for steel-fiber-reinforced concrete [34]. The relevant standards typically restrict the inclination range to $1.0 \le \cot(\theta) \le 2.5$. In addition, the concepts presented in NCHRP Report 655 [35], consistent with the AASHTO LRFD specifications [36] for shear and torsion assessment, recommend that θbe evaluated more explicitly, with an upper bound of $\cot(\theta) \le 1.8$ [36]. However, within the scope of ACI 318-19 [18] for RC members under torsion, a constant value of $\theta = 45^{\circ}$ is commonly adopted, whereas GB 50010 [19] does not explicitly use (θ) but instead introduces an equilibrium coefficient (ζ) to relate the contributions of transverse and longitudinal reinforcement. Moreover, the influence of the UHPC tensile contribution on the inclination angle (θ) is not explicitly considered in these standards.

In this section, a space-truss model is proposed to evaluate the strut inclination angle for UHPC beams under torsion (Figure 5). The model consists of inclined concrete compression struts, while the longitudinal reinforcement and the transverse reinforcement (stirrups) act as tensile ties in the longitudinal and vertical directions. The optimal inclination angle (θ) is determined based on force equilibrium and strain compatibility between the reinforcement and the concrete. Accordingly, the relationship between the forces in the stirrups and the longitudinal reinforcement can be established as follows:

$$\left(F_{sl} + F_{fl}\right)\tan\theta = \left(F_{st} + F_{ft}\right)\cot\theta \quad (23)$$

where F_{st} is the tensile force in the transverse reinforcement (stirrups) acting perpendicular to the beam axis; F_{sl} is the tensile force in the longitudinal reinforcement acting along the beam axis; and F_{ft} and F_{fl} are the tensile forces contributed by UHPC in the vertical and longitudinal directions, respectively. These forces are determined as follows:

$$F_{st} = \frac{A_{st} f_{yt}}{s} \quad (24)$$

$$F_{ft} = f_{ft,tu} t_d u \quad (25)$$

$$F_{sl} = \frac{A_{sl} f_{yl}}{P_h} \quad (26)$$

$$F_{fl} = f_{fl,tu} t_d u \quad (27)$$

From the force equilibrium condition in Eq. (23), the following expression is obtained:

$$\tan\theta = \sqrt{\frac{F_{st} + F_{ft}}{F_{sl} + F_{fl}}} \quad (28)$$

By substituting Eqs. (24)-(27) into Eq. (28), the optimal inclination angle is determined as follows:

$$\theta = \arctan\sqrt{\frac{F_{st}+F_{ft}}{F_{sl}+F_{fl}}} = \arctan\sqrt{\frac{\frac{A_{st}f_{yt}}{s}+f_{ft,tu}t_d u}{\frac{A_{sl}f_{yl}}{P_h}+f_{fl,tu}t_d u}} \quad (29)$$

4. Verification and discussion

This section evaluates the predictive performance of the ACI 318-19 [18] provisions, the GB 50010 [19] approach, and the proposed modified space-truss model (MSTM) against the experimental database of 40 UHPC beams tested under pure torsion [3, 12, 17, 20, 37]. The selected beams cover a broad range of longitudinal and transverse reinforcement ratios (ρ_{sl} and ρ_{st}), geometric proportions (b, h), and steel-fiber contents (ρ_f). The compressive strength of UHPC in the database varies from 116 to 205 MPa, while the fiber volume fraction ranges from 0.50 % to 3.5 %, thereby ensuring that the assessment reflects diverse material and detailing conditions. The comparisons are presented using parity plots of calculated versus experimental ultimate torsional capacities and the corresponding distributions of the calculated-to-experimental ratio ($T_{u,cal}/T_{u,exp}$), with ±20 % bounds adopted as a practical indicator of design-level accuracy.

Figure 6 compares the ACI 318-19 [18] torsion predictions with the experimental capacities of UHPC beams. A pronounced underestimation is observed. In the parity plot (Figure 6a), almost all data points fall well below the 1:1 line, and the majority lie outside the lower (−20 %) bound, indicating that the ACI-based model is not only conservative but also unable to capture the level of UHPC torsional resistance. The ratio plot (Figure 6b) further confirms this strong bias, with $T_{u,cal}/T_{u,exp}$ mostly far below unity across the full experimental capacity range. Quantitatively, the mean value (MV) of $T_{u,cal}/T_{u,exp}$ is 0.28 with a standard deviation (SD) of 0.14, demonstrating severe conservatism coupled with notable scatter. No clear improvement is observed at higher torsional capacities; the calculated-to-experimental ratios remain low even for specimens with larger $T_{u,exp}$, suggesting that the conservative bias is inherent to the approach. Mechanistically, this discrepancy is attributed to the fact that ACI torsion provisions are primarily calibrated for conventional reinforced concrete and do not explicitly represent the post-cracking tensile contribution of UHPC associated with fiber bridging. Consequently, the additional torsion-carrying contribution of UHPC after cracking is neglected, resulting in systematic underprediction.

Figure 7 presents the comparison between the GB 50010 [19] predictions and the experimental results. Compared with ACI 318-19, GB 50010 provides a clear improvement in accuracy: data points are generally closer to the 1:1 line and many results fall within the ±20 % bounds (Figure 7a). The ratio plot (Figure 7b) indicates that the predictions are still mostly below unity, confirming a persistent conservative tendency, but with a substantially reduced magnitude of underestimation. The MV of $T_{u,cal}/T_{u,exp}$ increases to 0.76 with a SD of 0.14, indicating improved agreement and moderate scatter over the investigated capacity range. Nevertheless, Figure 7 also suggests that the conservatism is not uniform across specimen series: a group of higher-capacity beams remains underestimated, while a limited number of data points approach or slightly exceed unity. This behavior is consistent with the fact that the GB torsion model is also established mainly for conventional reinforced concrete and only indirectly reflects UHPC post-cracking behavior, implying that further UHPC-oriented refinement is required.

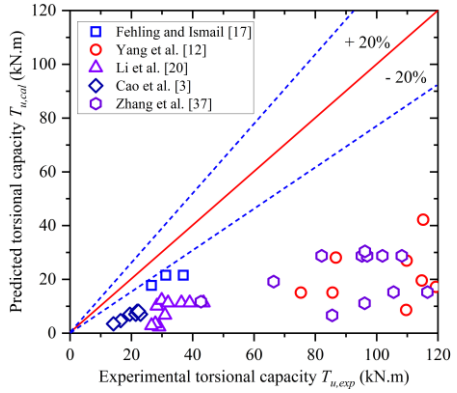

(a) Torsional capacity

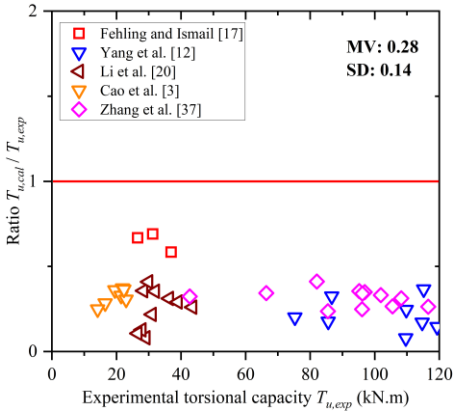

(b) Calculated-to-experimental ratio

Figure 6. Comparison between the ACI 318-19 based predictions and the experimental results.

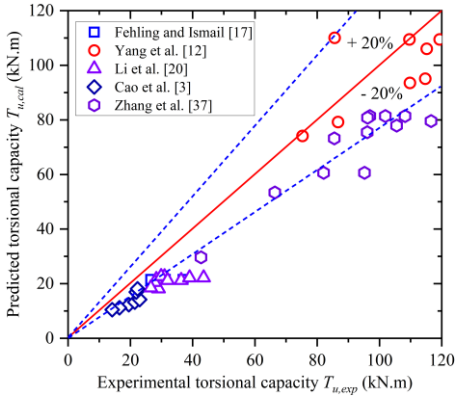

(a) Torsional capacity

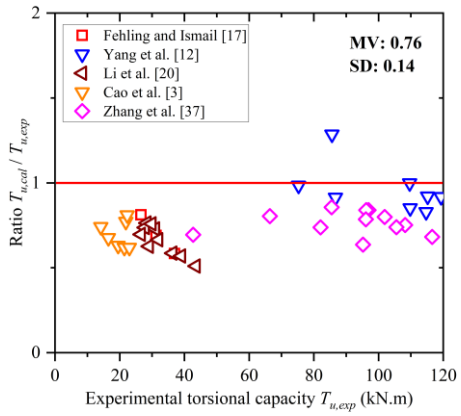

(b) Calculated-to-experimental ratio

Figure 7. Comparison between the GB50010 based predictions and the experimental results.

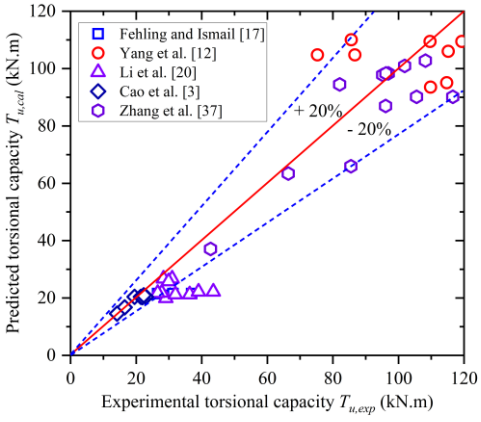

(a) Torsional capacity

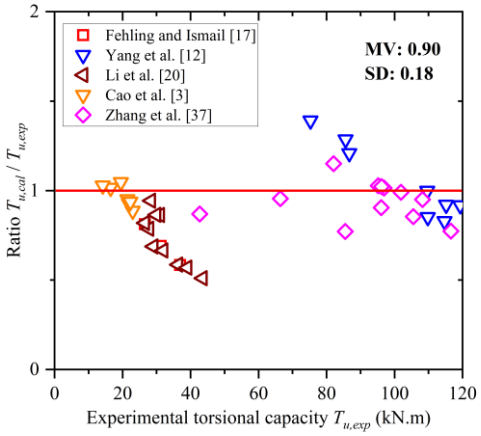

(b) Calculated-to-experimental ratio

Figure 8. Comparison between the MSTM predictions and the experimental results.

Figure 8 evaluates the proposed MSTM against the experimental database. The parity plot (Figure 8a) shows a marked improvement relative to the code-based approaches: predictions cluster tightly around the 1:1 line, and the majority of results lie within the ±20 % bounds across the full range of measured torsional capacities. The ratio plot (Figure 8b) confirms this improved accuracy, with $T_{u,cal}/T_{u,exp}$ distributed predominantly around unity. Statistically, the MV reaches 0.90 with a SD of 0.18, indicating a mild conservative bias with acceptable scatter for design-oriented estimation. The remaining deviations appear to be series-dependent: a subset of specimens at relatively low experimental capacities shows more pronounced underestimation, whereas several higher-capacity beams exhibit ratios close to or slightly above unity. These deviations are likely associated with variability in UHPC post-cracking tensile parameters (e.g., definition and identification of residual tensile strengths), fiber content and orientation effects, and reinforcement detailing among different test programs. Overall, the results demonstrate that explicitly accounting for UHPC post-cracking tensile stress transfer via equivalent longitudinal and transverse contributions, together with a refined strut inclination angle based on equilibrium and strain compatibility conditions, leads to a substantial reduction in global bias and improved robustness of torsional capacity predictions.

From a design perspective, direct application of conventional torsion provisions may lead to overly conservative designs for UHPC members, potentially limiting the efficient utilization of UHPC material benefits. The proposed MSTM offers a rational and practical alternative for estimating UHPC torsional capacity within the investigated parameter range, providing improved accuracy while maintaining a mildly conservative margin suitable for design use.

5. Conclusions

This study proposes a modified space-truss model (MSTM) for predicting the torsional strength of UHPC beams under pure torsion. The following conclusions can be drawn:

The proposed MSTM retains the mechanics-based framework of the three-dimensional space-truss and thin-walled tube idealization, while incorporating UHPC-specific mechanisms that are not explicitly addressed in conventional torsion provisions. In particular, the post-cracking tensile stress transfer provided by fiber bridging is represented through equivalent longitudinal and transverse tensile contributions, enabling a rational consideration of the tensile load-carrying capacity of UHPC after cracking. In addition, the concrete strut inclination angle is determined using equilibrium and strain-compatibility conditions rather than fixed code-recommended values, leading to improved internal force distribution and more consistent predictions across different reinforcement ratios and section sizes.

Validation against a database of 40 UHPC torsion tests confirms that ACI 318-19 is excessively conservative (MV = 0.28, SD = 0.14), whereas GB 50010 provides improved but still conservative estimates (MV = 0.76, SD = 0.14). In contrast, the proposed MSTM shows the best overall agreement with experiments, with most predictions close to the 1:1 line and largely within ±20 % bounds (MV = 0.90, SD = 0.18). These results indicate a mild conservative bias with acceptable scatter, supporting the use of the MSTM for design-oriented estimation of UHPC torsional capacity.

The present validation is limited to pure torsion and the specimens available in the collected database (predominantly rectangular sections). Future work should extend the model to combined actions (shear–torsion and flexure–torsion), other cross-sectional shapes, and standardized procedures for identifying post-cracking tensile parameters to further reduce uncertainty.

References

[1]. Cao, X., Ren, Y.-C., Zhang, L., Jin, L.-Z., & Qian, K. (2022). Flexural behavior of ultra-high-performance concrete beams with various types of rebar. *Composite Structures.* 292: 115674. doi:https://doi.org/10.1016/j.compstruct.2022.115674

[2]. Wang, Q., Song, H.-L., Lu, C.-L., & Jin, L.-Z. (2020). Shear performance of reinforced ultra-high performance concrete rectangular section beams. *Structures.* 27: 1184-1194. doi:https://doi.org/10.1016/j.istruc.2020.07.036

[3]. Cao, X. *et al.* (2023). Torsional capacity of ultra-high-performance concrete beams using rectangle stirrup. *Journal of Building Engineering.* 69: 106231. doi:https://doi.org/10.1016/j.jobe.2023.106231

[4]. Hsu, T. T. C. (1968). Torsion of Structural Concrete-Behavior of Reinforced Concrete Rectangular Members. *American Concrete Institute.* 18: 261-306. doi:10.14359/17572

[5]. S.M.R. Lopes, L. F. A. B. (2009). Twist behavior of high-strength concrete hollow beams-formation of plastic hinges along the length. *Engineering Structures.* 31(1): 134-149. doi:https://doi.org/10.1016/j.engstruct.2008.08.003

[6]. Rahal, K. N. (2013). Torsional strength of normal and high strength reinforced concrete beams. *Engineering Structures.* 56: 2206-2216. doi:https://doi.org/10.1016/j.engstruct.2013.09.005

[7]. Rao, T. D. G., & Seshu, D. R. (2003). Torsion of steel fiber reinforced concrete members. *Cement and Concrete Research.* 33(11): 1783-1788. doi:https://doi.org/10.1016/S0008-8846(03)00174-1

[8]. Fuad Okay, S. E. (2012). Torsional behavior of steel fiber reinforced concrete beams. *Construction and Building Materials.* 28(1): 269-275. doi:https://doi.org/10.1016/j.conbuildmat.2011.08.062

[9]. Karimipour, A., de Brito, J., Ghalehnovi, M., & Gencel, O. (2022). Torsional behaviour of rectangular high-performance fibre-reinforced concrete beams. *Structures.* 35: 511-519. doi:https://doi.org/10.1016/j.istruc.2021.11.037

[10]. Zhu, Y., Zhang, Y., Hussein, H. H., & Chen, G. (2020). Flexural strengthening of reinforced concrete beams or slabs using ultra-high performance concrete (UHPC): A state of the art review. *Engineering Structures.* 205: 110035. doi:https://doi.org/10.1016/j.engstruct.2019.110035

[11]. Xue, J., Briseghella, B., Huang, F., Nuti, C., Tabatabai, H., & Chen, B. (2020). Review of ultra-high performance concrete and its application in bridge engineering. *Construction and Building Materials.* 260: 119844. doi:https://doi.org/10.1016/j.conbuildmat.2020.119844

[12]. Yang, I.-H., Joh, C., Lee, J. W., & Kim, B.-S. (2013). Torsional behavior of ultra-high performance concrete squared beams. *Engineering Structures.* 56: 372-383. doi:https://doi.org/10.1016/j.engstruct.2013.05.027

[13]. Ibrahim, M. S., Gebreyouhannes, E., Muhdin, A., & Gebre, A. (2020). Effect of concrete cover on the pure torsional behavior of reinforced concrete beams. *Engineering Structures.* 216: 110790. doi:https://doi.org/10.1016/j.engstruct.2020.110790

[14]. Mohammed, T. J., Abu Bakar, B. H., & Muhamad Bunnori, N. (2016). Torsional improvement of reinforced concrete beams using ultra high-performance fiber reinforced concrete (UHPFC) jackets – Experimental study. *Construction and Building Materials.* 106: 533-542. doi:https://doi.org/10.1016/j.conbuildmat.2015.12.160

[15]. Zhou, J., Li, C., Feng, Z., & Yoo, D.-Y. (2022). Experimental investigation on torsional behaviors of ultra-high-performance fiber-reinforced concrete hollow beams. *Cement and Concrete Composites.* 129: 104504. doi:https://doi.org/10.1016/j.cemconcomp.2022.104504

[16]. Zhou, C., Wang, J., Jia, W., & Fang, Z. (2022). Torsional behavior of ultra-high performance concrete (UHPC) rectangular beams without steel reinforcement: Experimental investigation and theoretical analysis. *Composite Structures.* 299: 116022. doi:https://doi.org/10.1016/j.compstruct.2022.116022

[17]. Ekkehard Fehling, M. I. (2012). *Experimental Investigations on UHPC Structural Elements Subject to Pure Torsion*. Conference: Ultra-High Performance Concrete and Nanotechnology in ConstructionAt: Kassel, Germany.

[18]. ACI-318-19. (2019). *Building code requirements for structural concrete and commentary* American Concrete Institute, Farmington Hills, MI.

[19]. 50010, G. (2015). *Code for design of concrete structures*. China Architecture & Building Press: Beijing.

[20]. Li, C., Zhou, J., Ke, L., Yu, S., & Li, H. (2022). Failure mechanisms and loading capacity prediction for rectangular UHPC beams under pure torsion. *Engineering Structures.* 264: 114426. doi:https://doi.org/10.1016/j.engstruct.2022.114426

[21]. Imjong Kwahk, C. J., Jung Woo Lee. (2015). Torsional behavior design of UHPC box beams based on thin-walled tube theory. *Engineering and Technology Journal.* 7(3): 101-114. doi:http://dx.doi.org/10.4236/eng.2015.73009

[22]. Fib. (2010). *fib Model Code for Concrete Structures 2010*.

[23]. EN-1992-1-1:2004. (2004). *Design of Concrete Structures, Reinforced Concrete Standards; Reinforced Concrete Construction Standards*. European Committee for Standardization.

[24]. Rausch, E. (1929). *Berechnung des Eisenbetons gegen Verdrehung (Design of reinforced concrete in torsion)*. Berlin.

[25]. Lampert, P., Thurlimann, B. (1971). Torsion und Biegung von Stahlbetonbalken (Torsion and Bending of Reinforced Concrete Beams). *Bericht Nr 6506-2. Institut fur Baustatik, ETH Zurich*: 101.

[26]. CEB-FIP-90. (1990). *Comite Euro-International du Beton. CEB-FIP model code 1990*.Thomas Telford, London.

[27]. CAN3-A23.3-04. (2004). *Design of concrete structure for buildings*.Canadian Standards Association, Mississanga, Canada.

[28]. Bredt, R. (1896). Kritische Bemerkungen zur drehungselastizitat. *Z. Ver. Dtsch. Ing.* 40(28): 785-790.

[29]. Hsu, T. T., Mo, Y. L. (2010). *Unified theory of concrete structures*. Wiley, West Sussex, U.K.

[30]. Oettel, V. (2022). Steel fiber reinforced RC beams in pure torsion—Load-bearing behavior and modified space truss model. *Structural Concrete.* 24(1): 1348–1363. doi: https://doi.org/10.1002/suco.202200031

[31]. Mahshid Abdoli, D. M., Mohamadrza Eftekar, Alireza Saljoughian. (2024). Torsional strengthening of T-shaped RC members with FRP composites using EBROG method: Experimental investigation and analysis. *Construction and Building Materials.* 437: 136829. doi:https://doi.org/10.1016/j.conbuildmat.2024.136829

[32]. Mahshid Abdoli, D. M., Mohammadreza Eftekhar. (2024). Aggregate interlock and effective strain of FRP-strengthened flanged RC members subjected to torsion: Experimental evaluation and analytical modeling.

Construction and Building Materials. 437: 136865. doi:https://doi.org/10.1016/j.conbuildmat.2024.136865

[33]. Nguyen Vinh Sang , N. A. D., Nguyen Ngoc Thang. (2025). Analytical model for the torsional capacity of reinforced concrete beams strengthened with externally bonded frp sheets. *Journal of Materials and Construction*. 15(2): 21-29. doi:https://doi.org/10.54772/jomc.02.2025.794

[34]. Nguyen Vinh Sang , V. N. L., Le Thi Thanh Hieu, Vu Hoang Minh Khang. (2026). A modified strut and tie model for predicting the torsional strength of steel fiber-reinforced concrete beams. *Journal of Materials and Construction*. 16(2). doi:https://doi.org/10.54772/jomc.02.2026.1237

[35]. Abdul-Hamid Zureick, B. R. E., Andrzej S. Nowak, Dennis R. Mertz, Thanasis C. Triantafillou. (2010). *Recommended Guide Specification for the Design of Externally Bonded FRP Systems for Repair and Strengthening of Concrete Bridge Elements*.Transportation Research Board.

[36]. AASHTO-LRFD. (2014). *Bridge Design Specifications*.American Association of State Highway and Transportation Officials.

[37]. Zhang, Z., Xie, T.-Y., & Zhao, X.-Y. (2025). Torsional behavior of ultra-high-performance fiber-reinforced concrete beams: Testing, modeling and design recommendation. *Journal of Building Engineering*. 112: 113885. doi:https://doi.org/10.1016/j.jobe.2025.113885